Brain Structure and Function (2019) 224:1767–1779
https://doi.org/10.1007/s00429-019-01874-0

ORIGINAL ARTICLE

Distribution of excitatory and inhibitory axon terminals on the rat hypoglossal motoneurons

Sang Kyoo Paik[1] · Hong Il Yoo[2] · Seung Ki Choi[1] · Jin Young Bae[1] · Sook Kyung Park[1] · Yong Chul Bae[1]

Received: 30 July 2018 / Accepted: 11 April 2019 / Published online: 20 April 2019

Abstract

Detailed information about the excitatory and inhibitory synapses on the hypoglossal motoneurons may help understand the neural mechanism for control of the hypoglossal motoneuron excitability and hence the precise and coordinated movements of the tongue during chewing, swallowing and licking. For this, we investigated the distribution of GABA-, glycine (Gly)- and glutamate (Glut)-immunopositive (+) axon terminals on the genioglossal (GG) motoneurons by retrograde tracing, electron microscopic immunohistochemistry, and quantitative analysis. Small GG motoneurons (< 400 μm^2 in cross-sectional area) had fewer primary dendrites, significantly higher nuclear/cytoplasmic ratio, and smaller membrane area covered by synaptic boutons than large GG motoneurons (> 400 μm^2). The fraction of inhibitory boutons (GABA + only, Gly + only, and mixed GABA +/Gly + boutons) of all boutons was significantly higher for small GG motoneurons than for large ones, whereas the fraction of Glut + boutons was significantly higher for large GG motoneurons than for small ones. Almost all boutons (> 95%) on both small and large GG motoneurons were GABA +, Gly + or Glut +. The frequency of mixed GABA +/Gly + boutons was the highest among inhibitory boutons types for both small and large GG motoneurons. These findings may elucidate the anatomical substrate for precise regulation of the motoneuron firing required for the fine movements of the tongue, and also suggest that the excitability of small and large GG motoneurons may be regulated differently.

Keywords Hypoglossal motoneuron · Excitatory · Inhibitory · Presynaptic axon terminal · Immunohistochemistry · Electron microscopy

Introduction

Motoneurons in the hypoglossal (HG) nucleus control the muscle activity of the tongue during respiration, chewing, swallowing and licking (Sawczuk and Mosier 2001; Gestreau et al. 2005). The integration of excitatory and inhibitory synaptic inputs to HG motoneurons plays a crucial role for the control of the coordinated movements of the tongue (Liu et al. 2003; Horner 2009). Thus, glutamatergic synapses to HG motoneurons drive the rhythmical activity of HG motoneurons that underlie oral motor functions (Sharifullina et al. 2005; Steenland et al. 2008), and increased inhibitory synaptic input to HG motoneurons during sleep induces alteration of their firing that can lead to obstructive sleep apnea (Scrima et al. 1982; Krol et al. 1984; Yamuy et al. 1999; Horner 2009). Blocking of postsynaptic $GABA_A$ receptors on these motoneurons during hypercapnia also increases genioglossus muscle activity, leading to protrusion of the tongue (Morrison et al. 2003).

The HG motoneuron receives inhibitory synaptic input from 3 types of inhibitory synapses, pure GABAergic, pure glycinergic, and mixed GABA/glycinergic (Singer and Berger 2000; O'Brien and Berger 2001; Muller et al. 2006). Since the relevant postsynaptic receptors, $GABA_AR$ and GlyR, differ in their channel kinetics, the relative proportion of each type of inhibitory synapse on a motoneuron can influence its motor output and, consequently, the activity of the muscle innervated by it. Muller et al. (2004) have shown that the postsynaptic $GABA_AR$ and GlyR co-cluster

Sang Kyoo Paik, Hong Il Yoo, Seung Ki Choi contributed equally to this work.

✉ Yong Chul Bae
ycbae@knu.ac.kr

[1] Department of Anatomy and Neurobiology, School of Dentistry, Kyungpook National University, 188-1, 2-Ga, Samdeok-Dong, Jung-Gu, Daegu 700-412, South Korea

[2] Department of Anatomy and Neuroscience, College of Medicine, Eulji University, 77 Gyeryong-ro 771 beon-gil, Jung-Gu, Daejeon 34824, South Korea

at the majority of inhibitory synapses in the HG nucleus, suggesting that these are of the mixed type, but beyond that, detailed information on the distribution of excitatory and inhibitory synapses on the HG motoneurons, particularly on the genioglossal (GG) motoneurons that play a crucial role in maintaining airway patency during inspiration (Remmers et al. 1978), has been lacking.

To address this issue, we investigated the distribution of GABA-, Gly- and glutamate (Glut)-immunopositive axon terminals on the GG motoneurons by retrograde tracing, electron microscopic (EM) immunohistochemistry, and quantitative analysis. Since small and large motoneurons differ in the pattern of the synaptic input they receive (Destombes et al. 1992; Simon et al. 1996; Bae et al. 2002), we further compared the distribution of excitatory and inhibitory synapses on small vs. large GG motoneurons.

Materials and methods

All experimental procedures were reviewed and approved by the Kyungpook National University Intramural Animal Care and Use Committee.

Retrograde labeling of GG motoneurons

Experiments were performed on six male Sprague–Dawley rats weighing 290–310 g. The animals were anesthetized with sodium pentobarbital (40 mg/kg, i.p.), an incision was made on the skin of the neck below the jaw, and the digastric, mylohyoid and geniohyoid muscles were spread apart to reach the genioglossus muscle. One to three µl horseradish peroxidase (HRP, type IV, Toyobo, Tokyo, Japan; 30% in saline) was injected into multiple sites of the right genioglossus muscle with a 30-gauge needle glued to a Hamilton syringe, the surgical wound was repaired, and the rats were allowed to recover. After 16–24 h, the rats were deeply anesthetized with sodium pentobarbital (80 mg/kg, i.p.) and perfused through the heart with 100 ml of heparinized normal saline, followed by 500 ml of freshly prepared fixative, containing 2.5% glutaraldehyde, 1% paraformaldehyde, and 0.1% picric acid in phosphate buffer (PB; 0.1 M, pH 7.4).

Tissue preparation

The brain stem was removed, postfixed in the fixative used for perfusion for 2 h at 4 °C, and stored in PB. The 60 µm-thick serial transverse sections of the relevant region of brainstem were cut with a Vibratome. Retrogradely transported HRP was visualized according to the tungstate/tetramethylbenzidine protocol of Weinberg and van Eyck (1991) and stabilized with diaminobenzidine in PB (0.25 mg/ml, pH 6.0). Wet sections were examined under a light microscope and those containing HRP-labeled neurons in the ventral subdivision of the HG nucleus were further postfixed with 0.5% osmium tetroxide in PB (pH 6.0) for 40 min, dehydrated in graded alcohols, flat embedded in Durcupan ACM (Fluka, Switzerland) between strips of Aclar plastic film (EMS, Hatfield, PA, USA), and cured for 48 h at 60 °C. Chips containing multiple HRP-labeled GG motoneurons with prominent nucleoli were cut out of the wafers and glued onto blank blocks with cyanoacrylate. Serial thin sections were collected on formvar-coated single slot nickel grids.

Postembedding immunogold staining

Postembedding immunogold staining for GABA, Gly and Glut was performed following the method previously published from our laboratory (Paik et al. 2012a, b). Briefly, the grids were treated for 10 min in 1% periodic acid, to etch the resin, and for 15 min in 9% sodium periodate, to remove the osmium tetroxide. Sections were then washed in distilled water, transferred to tris-buffered saline containing 0.1% triton X-100 (TBST; pH 7.4) for 10 min, and incubated in 2% human serum albumin (HSA) in TBST for 10 min, to block non-specific binding of the primary antibodies. The grids were further incubated with rabbit polyclonal antisera against GABA (GABA 990, 1:800), Gly (glycine 290, 1:280) or Glut (Glu 607; 1:1,000) in TBST, containing 2% HSA for 3 h at room temperature. To eliminate cross-reactivity, the diluted antisera were preadsorbed overnight with glutaraldehyde (G)-conjugated amino acids (500 µM Glut-G for GABA, 300 µM β-alanine-G and 200 µM GABA-G for Gly, 300 µM glutamine-G, 100 µM aspartate-G, and 200 µM β-alanine-G for Glut; Ottersen et al. 1986). After extensive rinsing in TBST, grids were incubated in goat anti-rabbit IgG antibody coupled to 15 nm gold particles (1:25 in TBST containing 0.05% polyethylene glycol; BioCell, Cardiff, UK) for 3 h at room temperature. After a rinse in distilled water, the grids were counterstained with uranyl acetate and lead citrate, and examined on a Hitachi H-7500 electron microscope (Hitachi, Tokyo, Japan) at 80 kV accelerating voltage. Electron micrographs were taken using a DigitalMicrograph software driving a SC1000 camera (Gatan; Pleasanton, CA, USA) attached to the microscope. The images were saved as TIFF files, and brightness and contrast were adjusted with Photoshop 7.0 (Adobe Systems, San Jose, CA, USA).

Quantitative analysis

To measure the size of HRP-labeled GG motoneurons, light micrographs (×400) were obtained from flat embedded sections on a Zeiss Axioplan 2 microscope with an Exi digital camera (Q-imaging Inc., Surrey, CA), and saved as TIFF files. The cross-sectional areas of somata and nuclei of HRP-labeled GG motoneurons with visible nucleoli were

measured using a digitizing tablet and Image J software (v.1.45; NIH, Bethesda, MD, USA). Nuclear-cytoplasmic ratio (N/C ratio) was determined by dividing the area of the nucleus by the area of the soma.

The quantitative analysis of GABA+, Gly+ and Glut+ boutons was performed on eleven small (< 400 μm^2 in cross-sectional area) and thirteen large (> 400 μm^2, this value was chosen because of the apparent significant difference in the number of primary dendrites and N/C ratio between GG motoneurons with cross-sectional area below and above that value) HRP-labeled GG motoneurons in sections with visible nucleoli from 6 rats. Electron micrographs (×25,000) were taken along the entire somatic membrane in a series of thin sections incubated with GABA, Gly or Glut. To assess the immunoreactivity for GABA and Gly, the gold particle density, measured as the number of gold particles per μm^2, of each bouton was compared with that of its postsynaptic soma. Boutons were considered GABA- and/or Gly-immunopositive if the gold particle density for the respective antigen over the vesicle-containing areas of the bouton was at least five times the particle density in the corresponding postsynaptic region (this is the routinely used standard for distinguishing metabolic from transmitter GABA and glycine in axon terminals, Bae et al. 2002; Paik et al. 2012b). To assess the immunoreactivity for Glut, gold particle density of each bouton was compared to the average tissue density in 15–30 randomly selected areas adjacent to the somata of GG motoneurons and their apposing boutons (2 μm^2 each, a total area of 30–60 μm^2 per section). Boutons containing gold particles at a density larger than the mean + 2.576 S.D. of the average tissue density (significant difference at a 99% confidence level) were considered Glut-immunopositive. The immunogold labeling for GABA, glycine, and glutamate over mitochondrial and nuclear profiles was excluded from the analysis.

Measurements of boutons were also performed on electron micrographs (×25,000) taken along the entire somatic membrane in a single section of GG motoneurons with visible nucleoli, using a digitizing tablet and NIH image (v.1.45; NIH, Bethesda, MD, USA). A total of 156 boutons on 11 small GG motoneurons and 506 boutons on 13 large GG motoneurons were analyzed. The following parameters were recorded for each GG motoneuron: (1) perimeter and number of boutons apposing the somatic membrane, (2) mean length of bouton apposition, and (3) fraction of somatic membrane covered by boutons (synaptic covering percentage: total length of bouton apposition/perimeter × 100). Statistical analysis for differences between small and large GG motoneurons was performed by unpaired Student's *t* test. One caveat of the resulting numbers is that they can be used with confidence only for comparative purposes: we chose to not use a stereological approach, to simplify the analysis, and because in our experience, the number of boutons apposing the GG motoneuron somata and synaptic covering percentage are useful proxies in analyzing the differences in synaptic input between small and large GG motoneurons.

Antibody characterization

The antisera (a kind gift from Dr. Ottersen at the Centre for Molecular Biology and Neuroscience, University of Oslo, Norway) were raised according to the procedure of Storm-Mathisen et al. (1983), except that GABA, Gly and Glut were conjugated to bovine serum albumin with glutaraldehyde and formaldehyde instead of glutaraldehyde alone. They were characterized by spot-testing (Ottersen and Storm-Mathisen 1984; Kolston et al. 1992) and have been used routinely in our previous work (Paik et al. 2007, 2012a, b). Their specificity was confirmed on test sections consisting of "sandwiches" of rat brain macromolecule-glutaraldehyde complexes of amino acids including GABA, Gly and Glut (Ottersen 1989; Paik et al. 2007). Omission of the primary antisera or replacement with normal rabbit serum or preadsorption of the diluted anti-GABA serum with 200 μM GABA-G, the anti-Gly serum with 300 μM Gly-G, and the anti-Glut serum with 300 μM Glut-G, also abolished the specific immunostaining.

Results

At light microscopic (LM) examination, HRP-labeled GG motoneurons of various sizes (119.7–1243.1 μm^2 in cross-sectional area) were dense in the ventral and ventrolateral subdivisions of the HG nucleus (Fig. 1). Small GG motoneurons (< 400 μm^2 in cross-sectional area) had fewer primary dendrites and significantly higher nuclear/cytoplasmic ratio than large ones (> 400 μm^2: 0.32 ± 0.06 vs. 0.20 ± 0.03, $p < 0.001$).

At EM examination, HRP-labeled GG motoneurons were readily identifiable by the presence of crystalline or rod-shape deposits of HRP reaction product in the cytoplasm (Fig. 2). A total of 156 boutons apposing 11 small GG motoneurons (13.4 ± 2.9 boutons per motoneuron) and 506 boutons apposing 13 large GG motoneurons (38.9 ± 9.7 boutons per motoneuron) were analyzed. In a single section of a GG motoneuron, the number of boutons per GG motoneuron, the mean length of total bouton apposition, and the fraction of somatic membrane covered by boutons (synaptic covering percentage) were significantly higher for large GG motoneurons than for small GG motoneurons (Table 1). The majority (8/13) of large GG motoneurons but none of the small ones were contacted by boutons characterized by round vesicles and long subsynaptic cisterns (C boutons, Fig. 3).

Based on the immunogold staining for GABA, Gly and Glut on serial thin sections, the boutons apposing

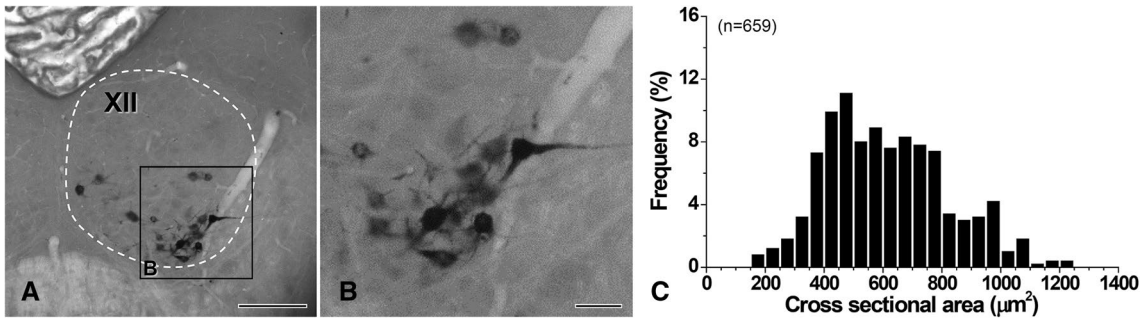

Fig. 1 Light micrographs showing HRP-labeled genioglossal (GG) motoneurons (**a**, **b**) and a histogram showing their size distribution (**c**). **a**, **b** HRP-labeled GG motoneurons are found in the ventrolateral subdivision of the hypoglossal nucleus (XII, outlined by a dashed line). **b** is an enlargement of the boxed area in **a**. "*n*" is the number of neurons analyzed. Scale bars = 200 μm in **a** and 50 μm in **b**

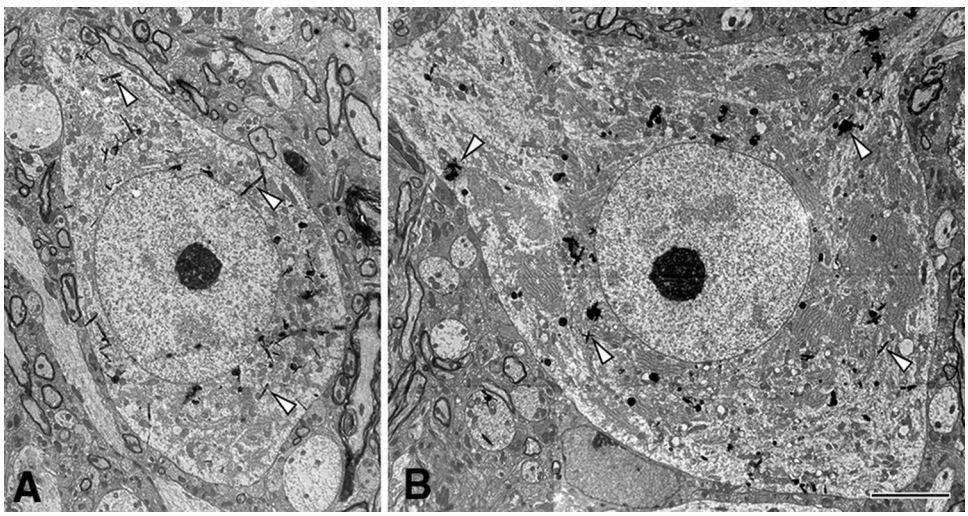

Fig. 2 Electron micrographs showing small (**a**) and large (**b**) genioglossal (GG) motoneurons labeled with retrogradely transported HRP (arrowheads). Note the apparent higher nuclear/cytoplasmic ratio in the small GG motoneuron comparted to the large one. Scale bar = 5 μm (applies also to **a**)

Table 1 Quantitative data (Mean ± SD) for boutons apposing somata of genioglossal (GG) motoneurons

Parameters	Small GG motoneurons	Large GG motoneurons
Number of motoneurons examined	11	13
Cross-sectional area of motoneurons (μm²)	252.1 ± 71.6[a]	637.6 ± 128.8
Perimeter (μm)	51.2 ± 6.7[a]	76.4 ± 13.6
Number of boutons/motoneuron	13.4 ± 2.9[a]	38.9 ± 9.7
Length of boutons apposition (μm)	1.0 ± 0.2[a]	1.3 ± 0.2
Synaptic covering (%)	26.5 ± 5.7[a]	67.8 ± 13.5

[a]Indicates statistically significant difference between small and large GG motoneurons (unpaired *t* test, $p < 0.05$)

somata of the GG motoneurons could be categorized as (1) immunopositive for GABA only (GABA + only), (2) immunopositive for Gly only (Gly + only), (3) immunopositive for both GABA and Gly (mixed GABA +/Gly +), (4) immunopositive for glutamate (Glut +), and (5) immunonegative for GABA, Gly or Glut (immunonegative bouton, Figs. 3, 4 and 5). The gold particle density for GABA in GABA + boutons (GABA + only and mixed GABA +/Gly + boutons) and for Gly in Gly + boutons (Gly + only and mixed GABA +/Gly + boutons) were 5.6–58.2 times and 5.0–22.9 times the background density, respectively. The gold particle density for Glut in Glut + boutons was 1.0–25.3 times average tissue density (Fig. 6). GABA + and/or Gly + boutons contained vesicles of various shape and showed, in favorable sections, synaptic contacts of symmetric type, whereas Glut + boutons contained round vesicles and showed asymmetric synaptic contacts.

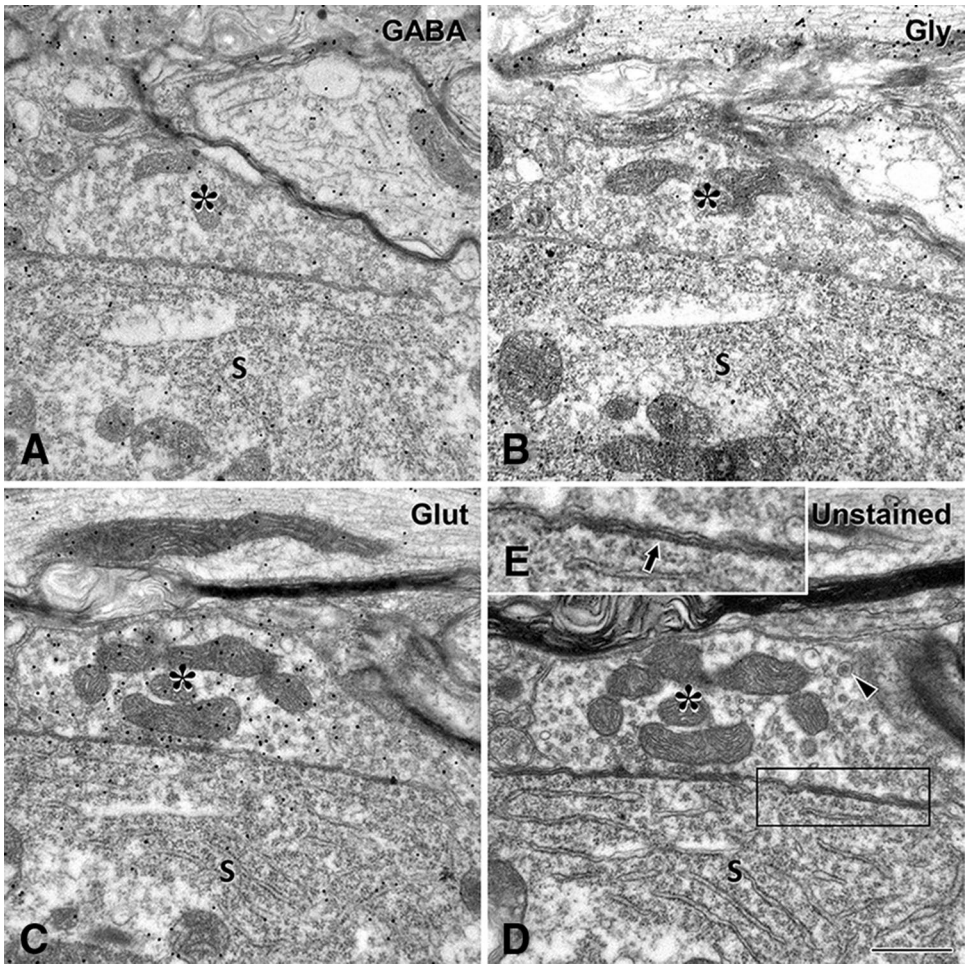

Fig. 3 Electron micrographs of adjacent thin sections incubated with antisera against GABA (**a**), glycine (Gly; **b**) and glutamate (Glut; **c**), and a section without immunogold staining (**d**, **e**), showing a C bouton (asterisk) making a synapse with a soma (S) of a large genioglossal motoneuron. The C bouton that is associated with a large subsynaptic cistern contains round vesicles and is immunopositive for glutamate but not for GABA or glycine. Retrogradely transported HRP labeling is present in the soma but out of view of this area. The arrowhead in **d** points to a dense core vesicle and the arrow in **e** points to a subsynaptic cistern. **e** is an enlargement of the boxed area in **d** to show the subsynaptic cistern more clearly. Scale bar = 500 nm (applies also to **a**–**c**)

The quantitative data for each bouton type are presented in Table 2 and Figs. 7, 8. Almost all (> 95%) boutons apposing GG motoneurons were GABA-, Gly- or Glut-immunopositive. The fraction of mixed GABA + /Gly + boutons of all boutons was the highest among the three inhibitory bouton types (GABA + only, Gly + only and mixed GABA + /Gly + boutons) for both small and large GG motoneurons. Each bouton type also showed significant differences between small and large GG motoneurons: (1) the fraction of inhibitory boutons (GABA and/or Gly + boutons: GABA + only, Gly + only and mixed GABA + /Gly + boutons) of all boutons was significantly higher for small GG motoneurons than for large ones, whereas the fraction of excitatory boutons (Glut +) was significantly higher for large GG motoneurons than for small ones, (2) the fraction of Gly + only boutons was significantly higher and the fraction of GABA + only boutons was significantly lower for large GG motoneurons than for small ones, and (3) the mean length of bouton apposition and synaptic covering percentage of all immunopositive bouton types were significantly higher for large GG motoneurons than for small ones.

Some gamma motoneurons in the lower cervical spinal cord have been reported to express GABA (Ito et al. 2008), which prompted us to test whether small GG motoneurons also contain GABA. Gold particle density for GABA in small GG motoneurons, large GG motoneurons, and GABA + boutons (apposing small GG motoneurons) was 1.1–3.3 times, 1.0–1.9 times, and 5.6–29.0 times, respectively, the particle density for GABA in boutons containing round vesicles and forming asymmetric synapses (background density in presumed excitatory synaptic boutons). Some small GG motoneurons (2/10), but none large GG motoneurons showed gold particle density three times higher than the background density (this cutoff value was used for distinguishing between GABA-immunopositive and GABA-immunonegative profiles by Sutherland et al. 2002). However, the particle density for GABA was much lower in both small and large GG motoneurons than in GABA + boutons (Fig. 9). These findings suggest that some small GG motoneurons may contain low levels of GABA, similar to that in the gamma motoneurons in the upper cervical spinal cord reported by Ito et al. (2008).

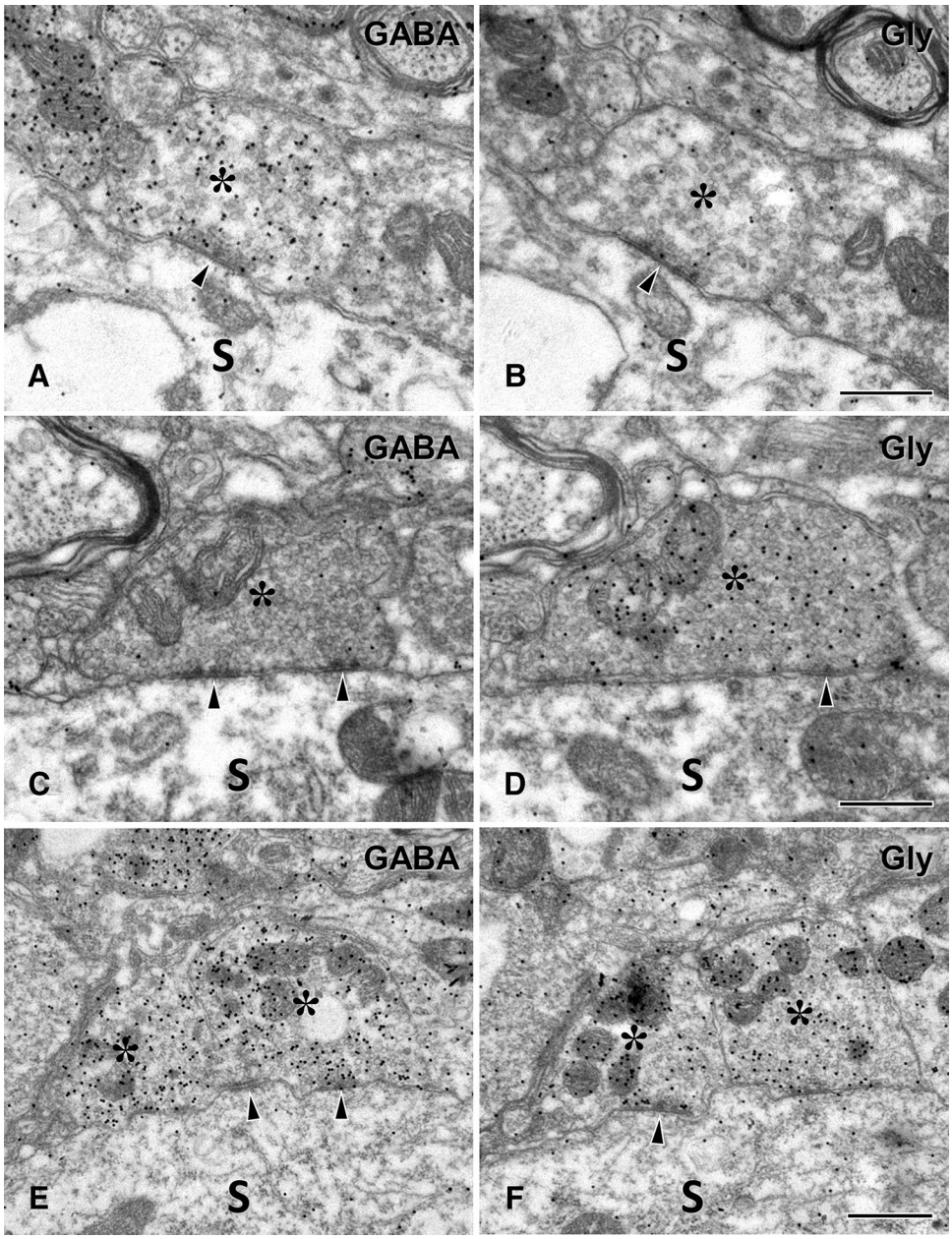

Fig. 4 Electron micrographs of pairs of adjacent thin sections incubated with antisera against GABA (**a**, **c**, **e**) and glycine (Gly; **b**, **d**, **f**) showing boutons (asterisks) making synapses (arrowheads) with somata (S) of large genioglossal motoneurons. Examples include boutons immunopositive for GABA alone (GABA + only bouton: **a**, **b**), glycine alone (Gly + only bouton: **c**, **d**), and for both GABA and glycine (mixed GABA +/Gly + bouton: **e**, **f**). Retrogradely transported HRP labeling is present in the soma but out of view in this area. Scale bars = 500 nm in **b**, **d**, **f** (applies to **a**, **c**, **e**, respectively)

Discussion

In the present study we report that: (1) the distribution pattern and morphological features of synapses onto small and large GG motoneurons are different, and (2) the frequency of mixed GABA +/Gly + boutons is the highest among the inhibitory bouton types in both small and large GG motoneurons. These findings may represent the anatomical substrate for the precise control of the movements of the tongue, and suggest that the excitability of small and large GG motoneurons may be regulated by different mechanisms.

Distribution of synapses onto small vs. large GG motoneurons

Small GG motoneurons had fewer primary dendrites, a significantly higher nuclear/cytoplasmic ratio, and much smaller synaptic covering percentage than large ones. In addition, C boutons, characterized by round vesicles and a large subsynaptic cisterns (Conradi 1969), frequently made contacts with large GG motoneurons and never with small ones. The distinctive features of small GG motoneurons described above, which are contrasted with those of large ones, are analogous to those of spinal and trigeminal gamma motoneurons (Destombes et al. 1992; Simon et al. 1996; Bae

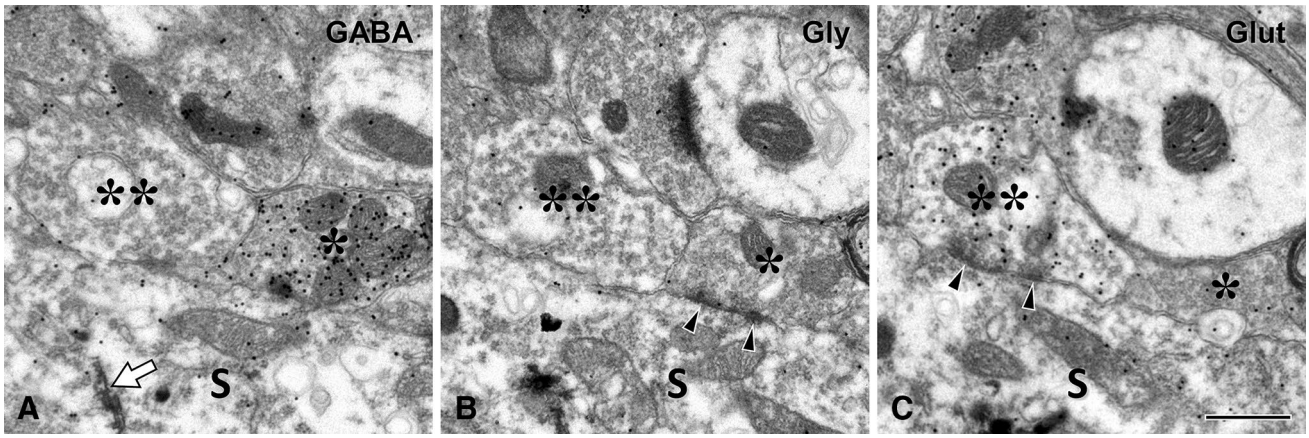

Fig. 5 Electron micrographs of adjacent thin sections incubated with antisera against GABA (**a**), glycine (Gly; **b**) and glutamate (Glut; **c**) showing boutons making synapses (arrowheads) with the soma (S) of a small genioglossal motoneuron. One of the boutons is immunopositive for GABA alone (GABA + only bouton: asterisk) and the other is immunopositive for glutamate (Glut + bouton: double asterisk). The arrow in **a** indicates reaction product of retrogradely transported HRP in the cytoplasm of the postsynaptic neuron. Scale bar = 500 nm in **c** (applies to **a**, **b**)

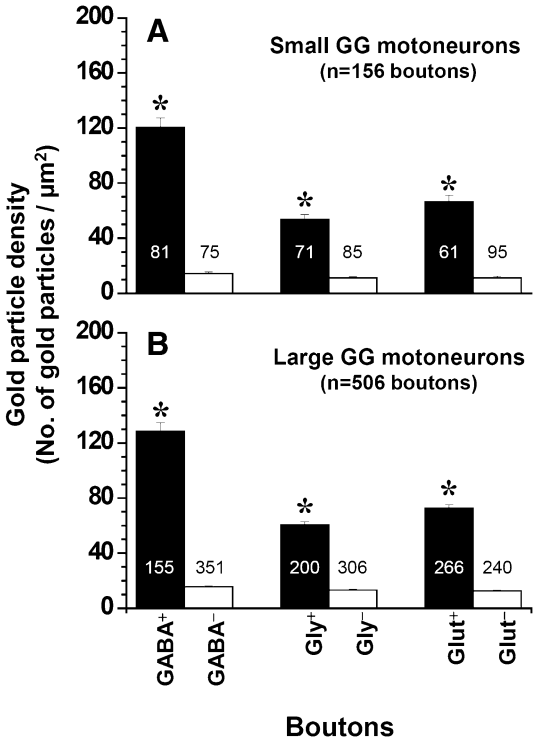

Fig. 6 Density of gold particles (mean ± standard error) over GABA-, glycine- and glutamate-immunopositive (+) and immunonegative (−) boutons apposing somata of small and large genioglossal (GG) motoneurons. Numbers within or over bars indicate the number of boutons examined for each bouton type. "n" indicates the total number of boutons examined (156 boutons for 11 small GG motoneurons and 506 boutons for 13 large GG motoneurons). Asterisks indicate statistically significant differences in gold particle density between immunopositive- and immunonegative-boutons (unpaired *t* test, $p < 0.001$)

et al. 2002). Considering the paucity of muscle spindles in the rat genioglossus muscle (O'Reilly and FitzGerald 1990), a few small GG motoneurons may be gamma motoneurons that innervate intrafusal fibers and are involved in the reflex activation of alpha motoneurons, whereas the majority of small GG motoneurons are likely to be alpha motoneurons that innervate extrafusal fibers. The size of the neuronal soma is correlated with the axonal size, conduction velocity, and amount of axoplasm, which in turn is determined by the diameter and the degree of branching of the axon (Lawson and Waddell 1991; Barret et al. 2009; Debanne et al. 2011; Park et al. 2016). Compared to large motoneurons, small motoneurons have smaller degree of axonal branching because they innervate fewer muscle fibers (Hall 2004; Berkowitz 2012) and are more likely to be involved in the control of precise movements (Brull 2014) and in maintaining the muscle tone (Buttner-ennever 2007). The function of the small GG motoneurons may thus be analogous to that of the small motoneurons innervating non-twitch muscle fibers in the extraocular muscles (Bach-Y-Rita et al. 1977; Buttner-ennever 2007).

The frequency of excitatory synapses was significantly higher for the large GG motoneurons than for the small ones, whereas that of inhibitory synapses was significantly higher for the small GG motoneurons than for the large ones. Gly + only boutons were significantly more frequent than GABA + only boutons onto large GG motoneurons, whereas the reverse was true about the two types of boutons onto the small GG motoneurons. The functional significance of these distribution patterns remains unclear. The existence of two kinds of GG motoneurons, small and large, with their distinct morphology and patterns of synaptic input, in addition to the paucity of muscle spindles in

Table 2 Quantitative data (Mean ± SD) for GABA +, Gly +, and Glut + boutons apposing somata of genioglossal (GG) motoneurons

Parameter	Small GG motoneurons	Large GG motoneurons
Number of motoneurons examined	11	13
Number of total boutons examined	156	506
GABA + only boutons		
Number/motoneuron (total)	1.5 ± 1.8 (17)[a]	1.3 ± 1.4 (17)
Percentage of all bouton profiles	10.8 ± 10.3[a]	3.5 ± 3.6
Length of boutons apposition (μm)	0.8 ± 0.3[a]	1.2 ± 0.4
Percentage of synaptic covering	2.5 ± 2.9	1.7 ± 1.6
Gly + only boutons		
Number/motoneuron (total)	0.8 ± 0.6 (7)[a]	4.8 ± 3.3 (62)
Percentage of all bouton profiles	6.1 ± 4.2[a]	12.6 ± 7.7
Length of boutons apposition (μm)	0.9 ± 0.4[a]	1.4 ± 0.4
Percentage of synaptic covering	1.1 ± 1.2[a]	8.7 ± 5.6
mixed GABA +/Gly + boutons		
Number/motoneuron (total)	5.8 ± 1.9 (64)[a]	10.6 ± 3.3 (138)
Percentage of all bouton profiles	40.4 ± 7.2[a]	28.3 ± 9.9
Length of boutons apposition (μm)	1.0 ± 0.3[a]	1.3 ± 0.2
Percentage of synaptic covering	10.6 ± 3.3[a]	18.3 ± 7.9
GABA + and/or Gly + boutons		
Number/motoneuron (total)	8.0 ± 2.8 (88)[a]	16.7 ± 3.7 (217)
Percentage of all bouton profiles	55.9 ± 10.4[a]	44.4 ± 10.9
Length of boutons apposition (μm)	1.0 ± 0.2[a]	1.3 ± 0.2
Percentage of synaptic covering	14.5 ± 4.2[a]	28.7 ± 9.4
Glut + boutons		
Number/motoneuron (total)	5.5 ± 1.6 (61)[a]	20.5 ± 9.0 (266)
Percentage of all bouton profiles	39.4 ± 9.1[a]	51.1 ± 12.0
Length of boutons apposition (μm)	1.0 ± 0.2[a]	1.4 ± 0.2
Percentage of synaptic covering	10.9 ± 3.9[a]	35.9 ± 10.4
GABA–/Gly–/Glut– boutons		
Number/motoneuron (total)	0.6 ± 0.8 (7)[a]	1.8 ± 0.9 (23)
Percentage of all bouton profiles	4.8 ± 6.8	4.6 ± 2.5
Length of boutons apposition (μm)	0.8 ± 0.3	1.4 ± 0.6
Percentage of synaptic covering	1.1 ± 1.5[a]	3.1 ± 1.9

Numbers in parentheses indicate the total number of boutons apposing 11 small and 13 large GG motoneurons

GABA + and/or Gly + boutons indicate GABA + only, Gly + only and mixed GABA +/Gly + boutons

[a]Indicates statistically significant difference between small and large GG motoneurons (unpaired *t* test, $p < 0.05$)

the genioglossus muscle (O'Reilly and FitzGerald 1990), may reflect a mechanism of control of the rat genioglossus muscle different from that of the jaw-closing (JC) and limb muscles.

The frequency of inhibitory boutons (GABA + and/or Gly + boutons) onto large GG motoneurons was lower than that onto JC alpha motoneurons (Bae et al. 2002), which may correlate to the electrophysiological differences between HG and JC motoneurons, where IPSPs are induced in JC motoneurons in the jaw opening phase during cortically induced fictive masticatory movement (Kubo et al. 1981; Chandler and Goldberg 1982; Goldberg et al. 1982), but not in HG motoneurons during cortically induced fictive tongue movement (Sahara et al. 1988).

GABA +, Gly +, and Glut + synapses onto GG motoneurons

Almost all (> 95%) boutons onto both small and large GG motoneurons were immunopositive for GABA, Gly or Glut, suggesting that the excitability of the GG motoneurons is regulated primarily by the three amino acid transmitters, analogous to the trigeminal and spinal motoneurons (Ornung et al. 1998; Shigenaga et al. 2005; Paik

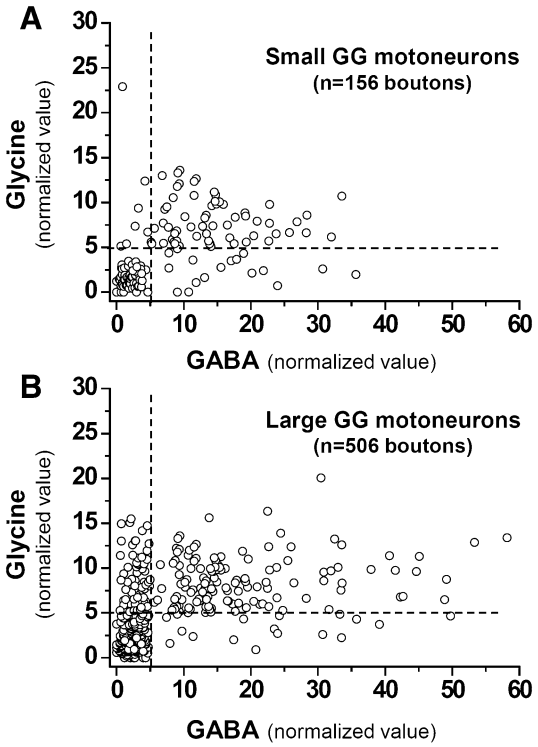

Fig. 7 Scatterplots of normalized values of gold particle density (gold particle density in bouton/background density) for GABA and glycine in boutons apposing somata of small and large genioglossal (GG) motoneurons. Background density was averaged from 15 to 30 randomly sampled 2 μm^2 square fields within the cytoplasm of the postsynaptic neuron. Dashed lines indicate the values below which the boutons were considered immunonegative for the respective antigen. "*n* =" indicates the total number of boutons examined (156 boutons for 11 small GG motoneurons and 506 boutons for 13 large GG motoneurons)

et al. 2012a). However, we also observed that GABA +, Gly + and Glut + boutons frequently contained dense core vesicles, known to be organelles for storage and release of neuropeptides and amines (Fried et al. 1985; Alvarez et al. 1993). That neuropeptides and amines are known to coexist with amino acid transmitters (Johnson 1994; Dal Bo et al. 2004) and can be expressed in premotoneurons that provide synaptic input to HG motoneurons (Henry and Manaker 1998; Rekling et al. 2000; Richardson and Gatti 2004; Zhou et al. 2014), raises the possibility that neuropeptides and/or amines are co-released with GABA +, Gly + and Glut + from boutons onto the GG motoneurons, providing a much more complex mechanism of regulation of the GG motoneurons' excitability than currently accepted.

The relative amount of GABA and Gly in mixed GABA +/Gly + boutons varied considerably, implying that the ratio of GABA to Gly may be different for individual mixed GABA +/Gly + boutons. We made an analogous observation for the terminals onto jaw-opening (JO) and JC motoneurons and onto the trigeminal mesencephalic neurons (Paik et al. 2007, 2012a, b). Since $GABA_A$R-mediated current has slow decay time and GlyR-mediated current has fast decay time (Jonas et al. 1998; Singer and Berger 2000; Nabekura et al. 2004), the release of various amounts of GABA and Gly from individual mixed GABA +/Gly + boutons can be involved in the fine temporal regulation of the postsynaptic membrane conductance (Rekling et al. 2000; Lu et al. 2008) or the precise shaping of the postsynaptic current (Jonas et al. 1998; Russier et al. 2002), in addition to strengthening of the postsynaptic inhibition by GABA and Gly corelease (Russier et al. 2002).

The frequency of mixed GABA +/Gly + boutons onto both small and large GG motoneurons was the highest among the three inhibitory bouton types. This is consistent with the results of an earlier immunohistochemical study in the hypoglossal nucleus, showing that the mixed $GABA_A$-glycine is a prominent type of inhibitory synapse, but is in contrast with another observation that Gly + only boutons are the most frequent type of bouton onto JC and JO motoneurons (Bae et al. 2002) and spinal motoneurons (Ornung et al. 1996). It is tempting to speculate that this reflects the more precise regulation of the postsynaptic neuron firing by mixed GABA +/Gly + boutons required for the fine movements of the tongue, compared to the relatively crude movements of the jaw or the limbs.

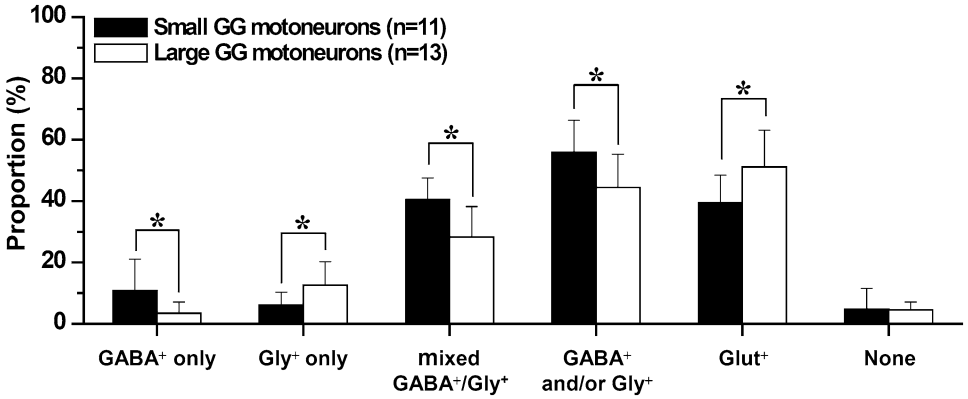

Fig. 8 Fraction (mean ± SD, %) of each immunopositive bouton type of all boutons apposing the somata of small and large genioglossal (GG) motoneurons. GABA + and/or Gly + boutons indicate GABA + only, Gly + only and mixed GABA +/Gly + boutons. The fractions of each immunopositive bouton type were significantly different between small and large GG motoneurons (asterisks, unpaired *t* test, $p < 0.05$)

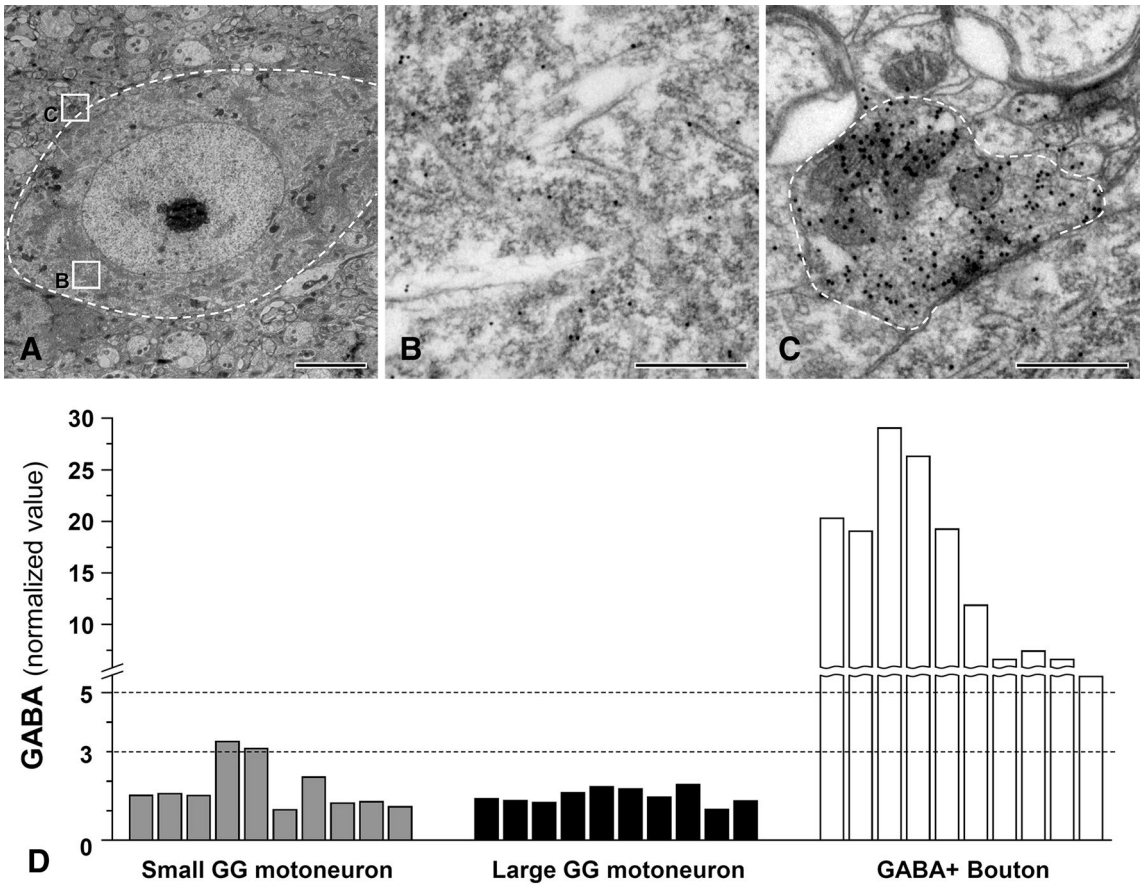

Fig. 9 Electron micrographs of thin sections incubated with antiserum against GABA showing gold particles coding for GABA in a small GG motoneuron (**a**, **b**) and a GABA + bouton contacting it (**a**, **c**), and a histogram (**d**) showing normalized values of gold particle density for GABA in 10 small GG motoneurons, 10 large GG motoneurons, and 10 GABA + boutons. The gold particle density for GABA is much lower in GG motoneurons than in GABA + boutons. "0" is the particle density for GABA in boutons containing round vesicles and forming asymmetric synapses (background density in presumed excitatory synaptic boutons). Note that two of the small GG motoneurons show gold particle density for GABA 3 times higher than background. The motoneuron in **a** and the GABA + bouton in C are outlined with a dashed line. **b** and **c** are enlargements of the boxed areas in **a**. Scale bar = 5 µm in **a** and 500 nm in **b**, **c**

The predominance of mixed GABA +/Gly + synapses onto GG motoneurons in the adult rat in the present study agrees with the report that postsynaptic $GABA_AR$ and GlyR co-cluster at the majority of inhibitory synapses onto the HG motoneurons in the adult mouse (Muller et al. 2004). However, it is in contrast to the finding, with light microscopy, that the frequency of GAD65 +/GlyT2 + presynaptic clusters is lower than that of the GlyT2 + clusters alone in the HG motoneurons of juvenile mice (Muller et al. 2006). This can be a true difference between juvenile and adult HG motoneurons, but can also be due to species differences or specific limitations of light vs. electron microscopy.

Source of synaptic input onto GG motoneuron

GG motoneurons receive afferent projections from several pontomedullary areas, including the medullary reticular formation, the trigeminal sensory nuclei, the solitary tract nucleus, and the pontine areas surrounding the trigeminal motor nucleus, which are associated with complex oral motor functions such as respiration, chewing, swallowing, and licking (Shepherd and Koch 1990; Peters et al. 1991; Fay and Norgren 1997; Chamberlin et al. 2007; Stanek et al. 2014; Travers 2015). Studies combining retrograde tracing and immunohistochemistry showed that HG motoneurons receive projections from glutamatergic premotoneurons, expressing vesicular glutamate transporter (VGLUT) 2, mainly in the medullary reticular formation (particularly its intermediate part), and partly in the Kölliker-Fuse nucleus (Travers et al. 2005; Yokota et al. 2011; Stanek et al. 2014), and from glutamatergic premotoneurons expressing VGLUT1 in the trigeminal mesencephalic nucleus (Zhang et al. 2003; Pang et al. 2006). HG motoneurons also receive projections from GABAergic and glycinergic premotoneurons in the pontomedullary reticular formation, supratrigeminal and trigeminal sensory nuclei, and the area near the

HG nucleus, including the nucleus of Roller (Li et al. 1997; Travers et al. 2005; Engelhardt et al. 2010; van Brederode et al. 2011). Despite this progress, however, the sources of GABAergic, glycinergic or glutamatergic input to the GG motoneurons remain poorly understood and warrant further investigation.

Acknowledgements The authors sincerely thank Dr. Juli Valtschanoff for helpful discussion and careful reading of the manuscript. We also sincerely thank Dr. O.P. Ottersen for the gift of the glutamate, GABA and glycine antibodies and the sandwich block for the test sections.

Funding This work was supported by the National Research Foundation of Korea (NRF) Grant funded by the Korea government (MSIT, NRF-2017R1A5A2015391, NRF-2017R1A2B2003561).

Compliance with ethical standards

Conflict of interest The authors declare that they have no conflict of interest.

Ethics approval All applicable international, national, and/or institutional guidelines for the care and use of animals were followed. All procedures performed in studies involving animals were in accordance with the ethical standards of the institution or practice at which the studies were conducted.

References

Alvarez FJ, Kavookjian AM, Light AR (1993) Ultrastructural morphology, synaptic relationships, and CGRP immunoreactivity of physiologically identified C-fiber terminals in the monkey spinal cord. J Comp Neurol 329:472–490

Bach-y-Rita P, Lennerstrand G, Alvarado J, Nichols K, McHolm G (1977) Extraocular muscle fibers: ultrastructural identification of iontophoretically labeled fibers contracting in response to succinylcholine. Invest Ophthalmol Vis Sci 16:561–565

Bae YC, Choi BJ, Lee MG, Lee HJ, Park KP, Zhang LF, Honma S, Fukami H, Yoshida A, Ottersen OP, Shigenaga Y (2002) Quantitative ultrastructural analysis of glycine- and gamma-aminobutyric acid-immunoreactive terminals on trigeminal alpha- and gamma-motoneuron somata in the rat. J Comp Neurol 442:308–319

Barret KE, Barman SM, Boitano S, Brooks H (2009) Excitable tissue: nerve. In: Barret KE, Barman SM, Boitano S, Brooks H (eds) Ganong's review of medical physiology, 23rd edn. McGraw-Hill Medical, New York, pp 79–92

Berkowitz A (2012) Motor Output from the Brain and Spinal Cord. In: eLS. https://doi.org/10.1002/9780470015902.a0000189.pub3

Brull SJ (2014) Physiology of neuromuscular transmission. In: Murray MJ, Harrison BA, Mueller JT, Rose SH, Wass CT, Wedel DJ (eds) Faust's anesthesiology review, 4th edn. Elsevier Saunders, Philadelphia, pp 98–99

Büttner-Ennever JA (2007) Anatomy of the oculomotor system. Dev Ophthalmol 40:1–14

Chamberlin NL, Eikermann M, Fassbender P, White DP, Malhotra A (2007) Genioglossus premotoneurons and the negative pressure reflex in rats. J Physiol 579:515–526

Chandler SH, Goldberg LJ (1982) Intracellular analysis of synaptic mechanisms controlling spontaneous and cortically induced rhythmical jaw movements in the guinea pig. J Neurophysiol 48:126–138

Conradi S (1969) Ultrastructure and distribution of neuronal and glial elements on the motoneuron surface in the lumbosacral spinal cord of the adult cat. Acta Physiol Scand Suppl 332:5–48

Dal Bo G, St-Gelais F, Danik M, Williams S, Cotton M, Trudeau LE (2004) Dopamine neurons in culture express VGLUT2 explaining their capacity to release glutamate at synapses in addition to dopamine. J Neurochem 88:1398–1405

Debanne D, Campanac E, Bialowas A, Carlier E, Alcaraz G (2011) Axon physiology. Physiol Rev 91:555–602

Destombes J, Horcholle-Bossavit G, Thiesson D, Jami L (1992) Alpha and gamma motoneurons in the peroneal nuclei of the cat spinal cord: an ultrastructural study. J Comp Neurol 317:79–90

Engelhardt JK, Silveira V, Morales FR, Pose I, Chase MH (2010) Serotoninergic control of glycinergic inhibitory postsynaptic currents in rat hypoglossal motoneurons. Brain Res 1345:1–8

Fay RA, Norgren R (1997) Identification of rat brainstem multisynaptic connections to the oral motor nuclei using pseudorabies virus. III. Lingual muscle motor systems. Brain Res Brain Res Rev 25:291–311

Fried G, Terenius L, Hokfelt T, Goldstein M (1985) Evidence for differential localization of noradrenaline and neuropeptide Y in neuronal storage vesicles isolated from rat vas deferens. J Neurosci 5:450–458

Gestreau C, Dutschmann M, Obled S, Bianchi AL (2005) Activation of XII motoneurons and premotor neurons during various oropharyngeal behaviors. Respir Physiol Neurobiol 147:159–176

Goldberg LJ, Chandler SH, Tal M (1982) Relationship between jaw movements and trigeminal motoneuron membrane-potential fluctuations during cortically induced rhythmical jaw movements in the guinea pig. J Neurophysiol 48:110–138

Hall WC (2004) Lower motor neuron circuits and motor control. In: Purves D, Augustine GJ, Fitzpatrick D, Hall WC, LaMantia A-S, McNamara JO, Williams SM (eds) Neuroscience, 3rd edn. Sinauer Associates, Sunderland, pp 371–392

Henry JN, Manaker S (1998) Colocalization of substance P or enkephalin in serotonergic neuronal afferents to the hypoglossal nucleus in the rat. J Comp Neurol 391:491–505

Horner RL (2009) Emerging principles and neural substrates underlying tonic sleep-state-dependent influences on respiratory motor activity. Philos Trans R Soc Lond B Biol Sci 364:2553–2564

Ito T, Hioki H, Nakamura K, Kaneko T, Iino S, Nojyo Y (2008) Some gamma-motoneurons contain gamma-aminobutyric acid in the rat cervical spinal cord. Brain Res 1201:78–87

Johnson MD (1994) Synaptic glutamate release by postnatal rat serotonergic neurons in microculture. Neuron 12:433–442

Jonas P, Bischofberger J, Sandkuhler J (1998) Corelease of two fast neurotransmitters at a central synapse. Science 281:419–424

Kolston J, Osen KK, Hackney CM, Ottersen OP, Storm-Mathisen J (1992) An atlas of glycine- and GABA-like immunoreactivity and colocalization in the cochlear nuclear complex of the guinea pig. Anat Embryol (Berl) 186:443–465

Krol RC, Knuth SL, Bartlett D Jr (1984) Selective reduction of genioglossal muscle activity by alcohol in normal human subjects. Am Rev Respir Dis 129:247–250

Kubo Y, Enomoto S, Nakamura Y (1981) Synaptic basis of orbital cortically induced rhythmical masticatory activity of trigeminal motoneurons in immobilized cats. Brain Res 230:97–110

Lawson SN, Waddell PJ (1991) Soma neurofilament immunoreactivity is related to cell size and fibre conduction velocity in rat primary sensory neurons. J Physiol 435:41–63

Li YQ, Takada M, Kaneko T, Mizuno N (1997) Distribution of GABAergic and glycinergic premotor neurons projecting to the facial and hypoglossal nuclei in the rat. J Comp Neurol 378:283–294

Liu X, Sood S, Liu H, Nolan P, Morrison JL, Horner RL (2003) Suppression of genioglossus muscle tone and activity during

reflex hypercapnic stimulation by GABA(A) mechanisms at the hypoglossal motor nucleus in vivo. Neuroscience 116:249–259
Lu T, Rubio ME, Trussell LO (2008) Glycinergic transmission shaped by the corelease of GABA in a mammalian auditory synapse. Neuron 57:524–535
Morrison JL, Sood S, Liu H, Park E, Nolan P, Horner RL (2003) GABAA receptor antagonism at the hypoglossal motor nucleus increases genioglossus muscle activity in NREM but not REM sleep. J Physiol 548:569–583
Muller E, Triller A, Legendre P (2004) Glycine receptors and GABA receptor alpha 1 and gamma 2 subunits during the development of mouse hypoglossal nucleus. Eur J Neurosci 20:3286–3300
Muller E, Le Corronc H, Triller A, Legendre P (2006) Developmental dissociation of presynaptic inhibitory neurotransmitter and postsynaptic receptor clustering in the hypoglossal nucleus. Mol Cell Neurosci 32:254–273
Nabekura J, Katsurabayashi S, Kakazu Y, Shibata S, Matsubara A, Jinno S, Mizoguchi Y, Sasaki A, Ishibashi H (2004) Developmental switch from GABA to glycine release in single central synaptic terminals. Nat Neurosci 7:17–23
O'Brien JA, Berger AJ (2001) The nonuniform distribution of the GABA(A) receptor alpha 1 subunit influences inhibitory synaptic transmission to motoneurons within a motor nucleus. J Neurosci 21:8482–8494
O'Reilly PM, FitzGerald MJ (1990) Fibre composition of the hypoglossal nerve in the rat. J Anat 172:227–243
Ornung G, Shupliakov O, Linda H, Ottersen OP, Storm-Mathisen J, Ulfhake B, Cullheim S (1996) Qualitative and quantitative analysis of glycine- and GABA-immunoreactive nerve terminals on motoneuron cell bodies in the cat spinal cord: a postembedding electron microscopic study. J Comp Neurol 365:413–426
Ornung G, Ottersen OP, Cullheim S, Ulfhake B (1998) Distribution of glutamate-, glycine- and GABA-immunoreactive nerve terminals on dendrites in the cat spinal motor nucleus. Exp Brain Res 118:517–532
Ottersen OP (1989) Quantitative electron microscopic immunocytochemistry of neuroactive amino acids. Anat Embryol (Berl) 180:1–15
Ottersen OP, Storm-Mathisen J (1984) Glutamate- and GABA-containing neurons in the mouse and rat brain, as demonstrated with a new immunocytochemical technique. J Comp Neurol 229:374–392
Ottersen OP, Storm-Mathisen J, Madsen S, Skumlien S, Stromhaug J (1986) Evaluation of the immunocytochemical method for amino acids. Med Biol 64:147–158
Paik SK, Bae JY, Park SE, Moritani M, Yoshida A, Yeo EJ, Choi KS, Ahn DK, Moon C, Shigenaga Y, Bae YC (2007) Developmental changes in distribution of gamma-aminobutyric acid- and glycine-immunoreactive boutons on rat trigeminal motoneurons. I. Jaw-closing motoneurons. J Comp Neurol 503:779–789
Paik SK, Kwak WK, Bae JY, Na YK, Park SY, Yi HW, Ahn DK, Ottersen OP, Yoshida A, Bae YC (2012a) Development of gamma-aminobutyric acid-, glycine-, and glutamate-immunopositive boutons on rat jaw-opening motoneurons. J Comp Neurol 520:1212–1226
Paik SK, Kwak MK, Bae JY, Yi HW, Yoshida A, Ahn DK, Bae YC (2012b) gamma-Aminobutyric acid-, glycine-, and glutamate-immunopositive boutons on mesencephalic trigeminal neurons that innervate jaw-closing muscle spindles in the rat: ultrastructure and development. J Comp Neurol 520:3414–3427
Pang YW, Li JL, Nakamura K, Wu S, Kaneko T, Mizuno N (2006) Expression of vesicular glutamate transporter 1 immunoreactivity in peripheral and central endings of trigeminal mesencephalic nucleus neurons in the rat. J Comp Neurol 498:129–141
Park SK, Lee DS, Bae JY, Bae YC (2016) Central connectivity of the chorda tympani afferent terminals in the rat rostral nucleus of the solitary tract. Brain Struct Funct 221:1125–1137
Peters A, Palay SL, Webster Hd (1991) The fine structure of the nervous system: neurons and their supporting cells, 3rd edn. Oxford University Press, New York
Rekling JC, Funk GD, Bayliss DA, Dong XW, Feldman JL (2000) Synaptic control of motoneuronal excitability. Physiol Rev 80:767–852
Remmers JE, deGroot WJ, Sauerland EK, Anch AM (1978) Pathogenesis of upper airway occlusion during sleep. J Appl Physiol Respir Environ Exerc Physiol 44:931–938
Richardson KA, Gatti PJ (2004) Genioglossal hypoglossal motoneurons contact substance P-like immunoreactive nerve terminals in the cat: a dual labeling electron microscopic study. Exp Brain Res 154:327–332
Russier M, Kopysova IL, Ankri N, Ferrand N, Debanne D (2002) GABA and glycine co-release optimizes functional inhibition in rat brainstem motoneurons in vitro. J Physiol 541:123–137
Sahara Y, Hashimoto N, Kato M, Nakamura Y (1988) Synaptic bases of cortically-induced rhythmical hypoglossal motoneuronal activity in the cat. Neurosci Res 5:439–452
Sawczuk A, Mosier KM (2001) Neural control of tongue movement with respect to respiration and swallowing. Crit Rev Oral Biol Med 12:18–37
Scrima L, Broudy M, Nay KN, Cohn MA (1982) Increased severity of obstructive sleep apnea after bedtime alcohol ingestion: diagnostic potential and proposed mechanism of action. Sleep 5:318–328
Sharifullina E, Ostroumov K, Nistri A (2005) Metabotropic glutamate receptor activity induces a novel oscillatory pattern in neonatal rat hypoglossal motoneurones. J Physiol 563:139–159
Shepherd GM, Koch C (1990) Appendix: Dendritic electrotonus and synaptic integration. In: Shepherd GM (ed) The synaptic organization of the brain, 3rd edn. Oxford University Press, New York, pp 439–473
Shigenaga Y, Moritani M, Oh SJ, Park KP, Paik SK, Bae JY, Kim HN, Ma SK, Park CW, Yoshida A, Ottersen OP, Bae YC (2005) The distribution of inhibitory and excitatory synapses on single, reconstructed jaw-opening motoneurons in the cat. Neuroscience 133:507–518
Simon M, Destombes J, Horcholle-Bossavit G, Thiesson D (1996) Postnatal development of alpha- and gamma-peroneal motoneurons in kittens: an ultrastructural study. Neurosci Res 25:77–89
Singer JH, Berger AJ (2000) Development of inhibitory synaptic transmission to motoneurons. Brain Res Bull 53:553–560
Stanek E 4th, Cheng S, Takatoh J, Han BX, Wang F (2014) Monosynaptic premotor circuit tracing reveals neural substrates for oromotor coordination. Elife 3:e02511
Steenland HW, Liu H, Horner RL (2008) Endogenous glutamatergic control of rhythmically active mammalian respiratory motoneurons in vivo. J Neurosci 28:6826–6835
Storm-Mathisen J, Leknes AK, Bore AT, Vaaland JL, Edminson P, Haug FM, Ottersen OP (1983) First visualization of glutamate and GABA in neurones by immunocytochemistry. Nature 301:517–520
Sutherland FI, Bannatyne BA, Kerr R, Riddell JS, Maxwell DJ (2002) Inhibitory amino acid transmitters associated with axons in presynaptic apposition to cutaneous primary afferent axons in the cat spinal cord. J Comp Neurol 452:154–162
Travers JB (2015) Oromotor nuclei. In: Paxinos G (ed) The rat nervous system, 4th edn. Academic Press, London, pp 223–245
Travers JB, Yoo JE, Chandran R, Herman K, Travers SP (2005) Neurotransmitter phenotypes of intermediate zone reticular formation projections to the motor trigeminal and hypoglossal nuclei in the rat. J Comp Neurol 488:28–47

van Brederode JF, Yanagawa Y, Berger AJ (2011) GAD67-GFP + neurons in the Nucleus of Roller: a possible source of inhibitory input to hypoglossal motoneurons. I. Morphology and firing properties. J Neurophysiol 105:235–248

Weinberg RJ, van Eyck SL (1991) A tetramethylbenzidine/tungstate reaction for horseradish peroxidase histochemistry. J Histochem Cytochem 39:1143–1148

Yamuy J, Fung SJ, Xi M, Morales FR, Chase MH (1999) Hypoglossal motoneurons are postsynaptically inhibited during carbachol-induced rapid eye movement sleep. Neuroscience 94:11–15

Yokota S, Niu JG, Tsumori T, Oka T, Yasui Y (2011) Glutamatergic Kolliker-Fuse nucleus neurons innervate hypoglossal motoneurons whose axons form the medial (protruder) branch of the hypoglossal nerve in the rat. Brain Res 1404:10–20

Zhang J, Pendlebury WW, Luo P (2003) Synaptic organization of monosynaptic connections from mesencephalic trigeminal nucleus neurons to hypoglossal motoneurons in the rat. Synapse 49:157–169

Zhou L, Wang ZY, Lian H, Song HY, Zhang YM, Zhang XL, Fan RF, Zheng LF, Zhu JX (2014) Altered expression of dopamine receptors in cholinergic motoneurons of the hypoglossal nucleus in a 6-OHDA-induced Parkinson's disease rat model. Biochem Biophys Res Commun 452:560–566